Optimal Stiffness Design to Limit Static and Dynamic Wind Responses of Tall Steel Buildings

CHUN-MAN CHAN

INTRODUCTION

With the continuing trend of constructing taller and slender buildings with higher strength materials and lighter structural systems, modern tall steel buildings are wind sensitive structures that are prone to serviceability problems. Two important serviceability limit states for tall building design are lateral deformations and motion perceptions under wind loads. Excessive lateral deformations have been found to cause windows to rack, non-structural partitions to crack and cladding to collapse. Exorbitant oscillations induced by turbulent wind have been known to cause occupant discomfort and even shatter windows.[1,2] The functions of tall buildings may be disrupted due to inadequate design for serviceability. Indeed, the design of tall slender buildings is generally governed by serviceability stiffness criteria rather than by ultimate strength safety requirements.

Stiffness design is the most challenging and difficult task in tall building design. When presented with a tall building to design, the structural engineer must select a suitable lateral load resisting system to resist wind and earthquake loads. Of the two lateral loads, the action of wind loads frequently determines the design of tall buildings. Common lateral load resisting systems for tall steel buildings are rigid frames, frames with shear trusses, outrigger trusses, tubular frames, and super diagonalized trusses. Often times, several preliminary structural alternatives are initially devised, and the choice of preliminary selection is then decided based on the engineer's experience, intuition and some approximate calculations. Once the topology of the lateral load resisting system is defined, the major effort is to size the structural members to satisfy both static and dynamic serviceability performance requirements. Since tall building structures usually consist of thousands of members and are very complex in nature, structural engineers are faced with the problem of how to distribute efficiently material throughout the structure to limit the static wind drifts and the dynamic wind vibrations.

Chun-Man Chan is assistant professor, department of civil and structural engineering, Hong Kong University of Science and Technology, Kowloon, Hong Kong.

The problem can become quite complex if a large scale three dimensional asymmetrical building structure exhibiting torsional swaying needs to be considered with multiple stiffness constraints under multiple loading conditions. Out of the many given structural members, one needs to determine which members are critical and to what extent the member sizes should be adjusted. Moreover, any modification of member sizes requires the structure to be reanalyzed. This traditional iterative resizing process is often tedious and time consuming.

With the emergence of structural optimization technology, the aforementioned resizing design process can be made in an automatic fashion and thus saving much design time. Structural optimization is nothing but a numerical tool that replaces the conventional trial-and-error design approach by a systematic goal-oriented design process. In such an optimization procedure, the numeric intensive tasks of the analysis-design cycle are formalized and the optimal member sizes are automatically sought while specified design constraints are simultaneously satisfied. In recent years, several design professionals[3-6] have developed ad hoc optimization software for sizing members of tall steel building frameworks to satisfy static wind drift. Although their methods are quite efficient, they are useful only for building structures with single displacement constraint problems. A number of researchers have developed formal optimization techniques for large-scale structures.[7-9] However, their efforts focus mostly on the optimization theory with little practical applications to realistic tall building structures.

Although it has long been recognized that structural optimization techniques have much to offer in engineering practice, the application of such technology for large scale building frameworks has been quite limited to date. Not until recently, the author has successfully developed an efficient optimization technique for the sizing design of tall practical building frameworks subject to multiple drift constraints and the use of discrete standard steel sections.[10,11] In this paper, the author intends to extend the optimization technology to include both static wind drift and dynamic natural period constraints. The design optimization problem is first explicitly defined and then the details of the optimization technique are developed. Two design examples are presented in the paper. The first example is a simple design problem that is used to illustrate the algorithm of the optimization technique. The second example is a full-scale, 50-story practical building structure through which the effectiveness and practicality of the automated optimal resizing technique are illustrated.

OPTIMAL DESIGN FORMULATION

Unlike the conventional design method, the formal optimization approach requires the designer to define explicitly a set of design variables, an objective function to be optimized and some explicit design constraints. In fact, a proper formulation of the optimal design problem is a key to good solutions. A good problem formulation should not only represent properly the current design problem but should also maintain a high level of accuracy during the evolution process of the design solution. Formulation details of the stiffness design of tall buildings are discussed as follows.

Design Variables and Objective

For a skeletal framework with a prescribed geometric layout, the design variables are the six basic cross sectional properties of each member, i.e., the axial area (A), two shear areas (A_Y, A_Z) and three moments of inertia (I_X, I_Y, I_Z). In this regard, a structure with N structural members should be theoretically described by $6N$ design variables. However, since commercially available standard steel sections are to be used for the design, section properties such as A_Y, A_Z, I_X, I_Y, I_Z can be accurately related to the cross sectional area A by certain functions through regressional analysis.[10] Linear relationships between reciprocal section properties are herein adopted and expressed as

$$\frac{1}{A_Y} = \frac{C_{AY}}{A} + C'_{AY} \tag{1a}$$

$$\frac{1}{A_Z} = \frac{C_{AZ}}{A} + C'_{AZ} \tag{1b}$$

$$\frac{1}{I_X} = \frac{C_{IX}}{A} + C'_{IX} \tag{1c}$$

$$\frac{1}{I_Y} = \frac{C_{IY}}{A} + C'_{IY} \tag{1d}$$

$$\frac{1}{I_Z} = \frac{C_{IZ}}{A} + C'_{IZ} \tag{1e}$$

where

C and C' = regressional constants derived under the assumption that the cross-section maintains within a constant shape group as it changes size

Figure 1 shows graphically the linear reciprocal relationships between the strong moment of inertia I_Z and cross sectional area A for W14, W24, W30 and W36 wide-flange sections from the AISC-LRFD design manual.[12] Using the regressional relationships, Equation 1, the six basic design variables (i.e., A, A_Y, A_Z, I_X, I_Y, I_Z) can be reduced to one cross sectional area variable (i.e., A) for each member.

If the topology of a building structural system is predefined, the design objective for a steel framework having $i = 1, 2, ..., N$ members can be expressed as

$$\sum_{i=1}^{N} w_i A_i \rightarrow \text{minimum} \tag{2}$$

where

A_i = the cross section area for member i
w_i = the corresponding material weight/cost coefficient per unit cross section area

Stiffness Design Constraints

A constraint is defined as a restriction that must be satisfied for a design to be acceptable or feasible. There are normally two types of serviceability performance constraints to be considered in tall building design.[13-16] The first type of con-

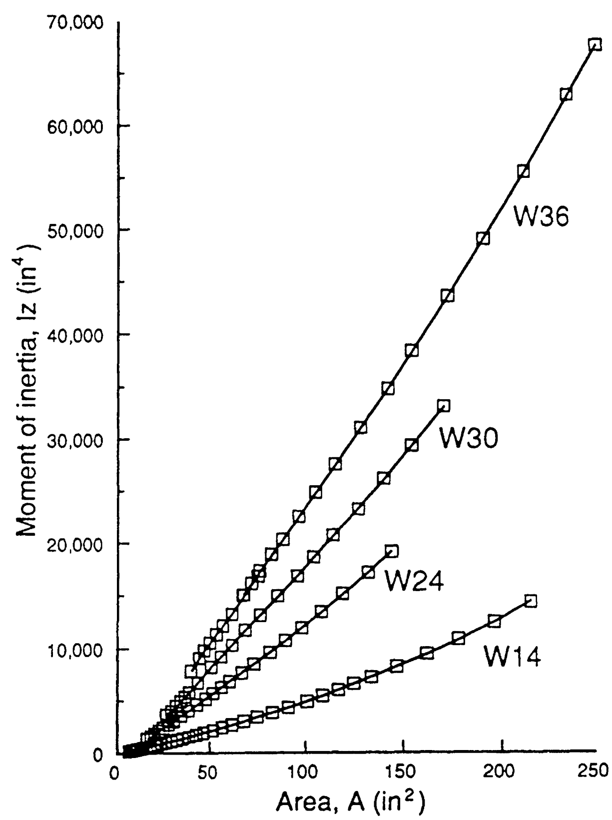

Fig. 1. Regressional relationships between strong moment of inertia I_z and cross-section area A for selected AISC W-shapes.

straints concerns with the static lateral deformations under wind loads. The second type deals with the dynamic wind motion perception.

1. Static Wind Drift.

Excessive magnitudes of lateral wind deflections may cause objectionable damage to nonstructural components or increase the chance of building instability. The static serviceability of a building can be secured by carefully controlling lateral deflections within certain allowable limits. Typically, two kinds of lateral deflections need be considered. One is the overall building drift, defined as the total lateral deflection at the roof top divided by the building height, H. Another is the interstory drift, which is the differential lateral translation of two adjacent floor levels per story height, h. While the overall building drift represents the average lateral translation of a building under wind effects, nonstructural damage is more dependent on interstory drift. The normally accepted range of drift ratio limits for buildings appears to be $\frac{1}{750}$ to $\frac{1}{250}$, with $\frac{1}{400}$ being typical.[13]

Consider a general 3D steel building framework having $i = 1, 2, ..., N$ members (or member fabrication groups), $j = 1, 2, ..., M$ storys, $k = 1, 2, ..., S$ column lines under $l = 1, 2, ..., L$ lateral loading conditions. The drift constraints can be expressed as

$$d_{kjl} = \frac{(\delta_{kjl} - \delta_{kj-1l})}{h_j} \le d_j^U$$

$$(k = 1, 2, ..., S);\ (j = 1, 2, ..., M);\ (l = 1, 2, ..., L) \tag{3a}$$

$$d_{kMl} = \frac{\delta_{kMl}}{H} \le d_H^U$$

$$(k = 1, 2, ..., S);\ (l = 1, 2, ..., L) \tag{3b}$$

Equation 3a defines interstory drift ratio d_{kjl}, where δ_{kjl} and δ_{kj-1l} are the lateral translations on a column line k at two adjacent j and $j-1$ floor levels under lateral loading condition l, h_j, is the jth story height and d_j^U is the allowable jth story drift limit; Equation 3b defines the overall building drift ratio d_{kMl}, where δ_{kMl} is the lateral translation on column line k at the top floor level M under lateral loading condition l, H is the building height and d_H^U is the allowable overall building drift limit. Note that the drift constraints Equation 3 are expressed in implicit form. In order to facilitate numerical solution of the design optimization problem, the drift constraints Equation 3 must be first expressed explicitly in terms of the design variables.

By the principle of virtual work, a displacement of interest δ can be expressed as

$$\delta = \sum_{i=1}^{N} \int_0^{L_i} \left(\frac{F_X f_X}{EA} + \frac{F_Y f_Y}{GA_Y} + \frac{F_Z f_Z}{GA_Z} + \frac{M_X m_X}{GI_X} + \frac{M_Y m_Y}{EI_Y} + \frac{M_Z m_Z}{EI_Z} \right)_i dx \tag{4}$$

where

L_i = length of member i
E, G = axial and shear elastic material moduli
A, A_y, A_z = axial and shear areas for the cross-section
I_x, I_y, I_z = torsional and flexural moments of inertia for the cross-section
$F_X, F_Y, F_Z,$
M_X, M_Y, M_Z = member forces and moments due to the actual wind loads
$f_X, f_Y, f_Z,$
m_X, m_Y, m_Z = member forces and moments due to a unit virtual load applied at the location of and in the sense of δ

Given a particular section type for each member, one can substitute the regressional relationships Equation 1 into Equation 4 to express instantaneously the displacement δ as explicit functions of the sizing variable A_i alone as

$$\delta(A_i) = \sum_{i=1}^{N} \left(\frac{c_i}{A_i} + c_i' \right) \tag{5}$$

where the virtual strain energy coefficients, c_i and the correction factors c_i' are respectively given by

$$c_i = \int_0^{L_i} \left(\frac{F_X f_X + M_Y m_Y C_{IY} + M_Z m_Z C_{IZ}}{E} + \frac{F_Y f_Y C_{AY} + F_Z f_Z C_{AZ} + M_X m_X C_{IX}}{G} \right)_i dx \tag{6a}$$

$$c_i' = \int_0^{L_i} \left(\frac{M_Y m_Y C_{IY}' + M_Z m_Z C_{IZ}'}{E} + \frac{F_Y f_Y C_{AY}' + F_Z f_Z C_{AY}' + M_X m_X C_{IX}'}{G} \right)_i dx \tag{6b}$$

As both the interstory drift constraints Equation 3a and the overall drift constraints Equation 3b are similar to each other, they can be simplified collectively into one single type of constraints for convenience of future discussion. The subscript (k, j, l) in the drift constraints Equation 3 can be changed to a single subscript d to represent the dth constraint in a collective set of N_d drift constraints, where N_d is the total number of interstory and overall building drift constraints for an M-story framework having concern for drift control of S column lines under L lateral loading conditions. Using the explicit displacement expression Equation 5, the drift constraints Equation 3 can be expressed in terms of the design variable A_i as

$$d_d = \sum_{i=1}^{N} \left(\frac{e_{id}}{A_i} + e'_{id} \right) \le d_d^U \ (d = 1, 2, ..., N_d) \tag{7}$$

where for interstory drifts,

$$e_{id} = \frac{c_{ikjl} - c_{ikj-1l}}{h_j}; \ e_{id}' = \frac{c'_{ikjl} - c'_{ikj-1l}}{h_j} \tag{8a, b}$$

and for overall building drifts,

$$e_{id} = \frac{c_{ikMl}}{H}; \ e'_{id} = \frac{c'_{ikMl}}{H} \tag{8c, d}$$

2. Wind-Induced Vibrations

It is widely accepted that wind-induced acceleration has become the standard for evaluation of motion perception in buildings.[15,16] Semi-empirical formulas have been derived from numerous wind tunnel studies to predict the acceleration responses of buildings in an urban environment. These formulas are expressed in terms of the wind velocity, the building's shape, damping ratio, mass and fundamental natural periods.[2,17] Wind-induced accelerations can be reduced by changing the building shape to maintain better aerodynamic stability, but unfortunately this is often beyond the control of the engineer. In practice, the mass of a building is hardly variant and it has not been common to design damping into a structural system. A common approach to suppress wind-induced vibrations remains to limit the natural periods.[18]

Using the Rayleigh method, the fundamental circular frequency of vibration ω for an undamped structure can be found by equating the maximum kinetic energy of the system at zero displacement to the work done by the inertia forces as the system moves from zero to maximum displacement as follow:

$$\frac{1}{2}\omega^2\phi^T M\phi \text{ (kinetic energy)}$$

$$= \frac{1}{2}\phi^T F \text{ (work done by inertia forces)} \tag{9a}$$

$$\Rightarrow \omega^2 = \frac{\phi^T F}{\phi^T M\phi} = \frac{\phi^T K\phi}{\phi^T M\phi} = \frac{K^*}{M^*} \tag{9b}$$

where

M, M^* = structure mass matrix and generalized mass
K, K^* = structure stiffness matrix and generalized stiffness
ϕ = the computed mode shape under the inertia force matrix F

Initially, if the structure has circular frequency ω_0 and mode shape ϕ_0, the inertia force F can be obtained as $\omega_0^2 M\phi_0$. For an undamped skeletal framework, the external work done by inertia force F is equal to the total internal work W represented by the total sum of internal strain energy for all members as

$$W = \sum_{i=1}^{N} \int_0^{L_i} \left(\frac{F_X^2}{EA} + \frac{F_Y^2}{GA_Y} + \frac{F_Z^2}{GA_Z} + \frac{M_X^2}{GI_X} + \frac{M_Y^2}{EI_Y} + \frac{M_Z^2}{EI_Z} \right)_i dx \tag{10}$$

where

$F_X, F_Y, F_Z,$
M_X, M_Y, M_Z = internal member forces and moments due to the external inertia loading condition, F

Using again the linear regression section relationships Equation 1, the total internal work Equation 10 can be expressed as explicit functions of the sizing variables A_i alone as

$$W(A_i) = \sum_{i=1}^{N} \left(\frac{e_{i\tau}}{A_i} + e'_{i\tau} \right) \tag{11}$$

where

τ = the fundamental mode of vibration
$e_{i\tau}$ and $e_{i\tau}'$ = are respectively given by

$$e_{i\tau} = \int_0^{L_i} \left(\frac{F_X^2 + M_Y^2 C_{IY} + M_Z^2 C_{IZ}}{E} + \frac{F_Y^2\, C_{AY} + F_Z^2\, C_{AZ} + M_X^2 C_{IX}}{G} \right)_i dx \tag{12a}$$

$$e'_{i\tau} = \int_0^{L_i} \left(\frac{M_Y^2 C'_{IY} + M_Z^2 C'_{IZ}}{E} + \frac{F_Y^2\, C'_{AY} + F_Z^2\, C'_{AY} + M_X^2 C'_{IX}}{G} \right)_i dx \tag{12b}$$

By definition, the natural period T is inversely related to the circular frequency ω as

$$T = \frac{2\pi}{\omega} \tag{13}$$

To limit the natural period T, one can increase ω by increasing the structure stiffness according to Equations 9 and 13. If one assumes temporarily constant initial inertia force F such that the internal member forces and moments are invariant, an increase in the structure stiffness can be achieved by increasing member sizes and thus reducing the internal work W. Assuming that the initial mode shape ϕ_o, inertia force F and structure mass M are invariant, one can limit the natural period T by the following explicit equivalent design constraint on internal work as

$$W(A_i) = \sum_{i=1}^{N} \left(\frac{e_{i\tau}}{A_i} + e'_{i\tau} \right) \le W^U \tag{14}$$

where the allowable work limit W^U can be shown equal to $(T^U / T_o)^2 (W_o)$ in which

T^U = targeted natural period
T_o = initial natural period
W_o = initial strain energy for the framework having the original member sizes

Under the influence of dynamic wind loads, tall buildings vibrate in the alongwind, acrosswind and torsional directions. Normally, there is one natural period to be limited respectively in each of these three wind sensitive directions, i.e. two translational and one torsional mode of vibrations. While slight modifications on the Rayleigh method are needed to obtain a higher mode shape and frequency,[19] the same form of explicit strain energy constraints as given in Equation 14 can be expressed for ($\tau = 1, 2, ..., N_\tau$) multiple natural period constraints as

$$W_\tau(A_i) = \sum_{i=1}^{N} \left(\frac{e_{i\tau}}{A_i} + e'_{i\tau} \right) \leq W_\tau^U \; (\tau = 1, 2, ..., N_\tau) \quad (15)$$

where

N_τ = total number of natural period constraints

Recognizing the fact that the explicit lateral drift Equation 7 and equivalent period constraint Equation 15 are very much alike, one can express collectively the stiffness design optimization problem in terms of sizing variables A_i as follows:

Minimize:

$$\sum_{i=1}^{N} w_i A_i \quad (16a)$$

subject to:

$$g_s(A_i) = \sum_{i=1}^{N} \left(\frac{e_{is}}{A_i} + e'_{is} \right) \leq g_s^U \; (s = 1, 2, ..., N_s) \quad (16b)$$

$$A_i^L \leq A_i \leq A_i^U \; (i = 1, 2, ..., N) \quad (16c)$$

Equation 16b denotes the stiffness constraints, where the constraint g_s with subscript $s = 1, 2, ..., N_d$ represents the static drift constraint in which $g_s^U = d_d^U$ as given in Equation 7; the constraint g_s with subscript $s = N_d + 1, ..., N_d + N_\tau$, represents the period constraint in which $g_s^U = W_\tau^U$ as given in Equation 15. In the case of having a set of multiple drift and period constraints, the value N_s represents the total number of stiffness design constraints, i.e. equal to $N_d + N_\tau$. Equation 16c specifies each design variable A_i to be selected from its lower bound size A_i^L and upper bound size A_i^U.

OPTIMIZATION TECHNIQUE

Upon formulating the design optimization problem for serviceability requirements of tall steel building framework, the next task is to apply a suitable method to solve the problem. A rigorously derived Optimality Criteria (OC) method, which has been shown computationally very efficient for large-scale structures is employed.[10,11] The OC method first involves the derivation of a set of necessary optimality criteria for the design. Then, a recursive algorithm is applied to resize the structure to satisfy the optimality conditions and thus indirectly optimize the structure. The basic essence of the OC technique is herein presented in this paper. Further details of the technique can be found in references 10 and 11.

Optimality Criteria

In classical optimization theory, the necessary optimality criteria for the constrained optimal design problem (Equation 16) can be obtained indirectly by first converting the constrained problem to an unconstrained Lagrangian function and then solving for the stationary condition of the Lagrangian function. Temporarily omitting the sizing constraints Equation 16c, the unconstrained Lagrangian function can be formulated as,[21-24]

$$L(A_i, \lambda_s) = \sum_{i=1}^{N} w_i A_i + \sum_{s=1}^{N_s} \lambda_s \left[\sum_{i=1}^{N} \left(\frac{e_{is}}{A_i} + e'_{is} \right) - g_s^U \right] \quad (17)$$

The first part of the Lagrangian function describes the structure weight, whereas the second part involves the design constraints multiplied by their corresponding Lagrange multipliers, λ_s. For minimization problems, the Lagrange multipliers must be positive for active constraints (i.e. $g_s = g_s^U$) or equal to zero for inactive constraints (i.e. $g_s < g_s^U$). Differentiating the Lagrangian function Equation 17 with respect to the design variables A_i and setting the derivative to zero, one can obtain the following necessary conditions at the optimum as

$$w_i + \sum_{s=1}^{N_s} \lambda_s \left(\frac{-e_{is}}{A_i^2} \right) = 0 \; (i = 1, 2, ..., N) \quad (18)$$

which can be rearranged to

$$\sum_{s=1}^{N_s} \lambda_s \frac{e_{is}}{w_i A_i^2} = 1 \; (i = 1, 2, ..., N) \quad (19)$$

The optimality criteria for the optimal design problem Equation 16 are shown in Equation 19, which have a significant physical meaning for design. Each Lagrangian multiplier, λ_s, can be interpreted as a sensitivity weighting factor which measures the importance of the corresponding sth constraint to the optimal design. The larger the value of λ_s, the more influential is the constraint to the optimum design. When a constraint does not affect the design, the corresponding λ_s diminishes to zero. The expression $e_{is}/w_i A_i^2$ in Equation 19 represents the strain energy per unit weight/cost, which is so called the strain energy density, for member i with respect to the sth constraint. Therefore, the optimality conditions Equation 19 specify that each member must contribute the same weighted amount of strain energy densities at the optimum. For the case of only one stiffness constraint, λ_s becomes a constant and the strain energy density, $e_{is}/w_iA_i^2$, for each member is uniform or, in fact, equal to $1/\lambda_s$.

Recursive Resizing Algorithm

Equations 19 are stationary conditions, equal to unity at the optimum, that can be used to derive a linear recursive relation for the active sizing variables A_i as follows,

$$A_i^{\nu+1} = A_i^{\nu}\left[1 + \frac{1}{\eta}\left(\sum_{s=1}^{N_s}\frac{\lambda_s e_{is}}{w_i A_i^2} - 1\right)_{\nu}\right] \quad (i = 1, 2, ..., N-\xi) \qquad (20)$$

where

η = step-size parameter that controls convergence of the recursive process

ν and

$\nu + 1$ = successive iterations

ξ = number of inactive members which are assigned to either their limiting sizes or fixed discrete sizes

In order to apply Equation 20 to find the new sizing variables $A_i^{\nu+1}$, the current values of the Lagrange multipliers λ_s^{ν} must first be determined. Considering the change of $(g_t^{\nu+1} - g_t^{\nu})$ in the tth constraint due to the change of $(A_i^{\nu+1} - A_i^{\nu})$ in the $(N-\xi)$ active sizing variables, the N_s Lagrange multipliers for the corresponding constraints can be expressed as a set of N_s simultaneous equations

$$\sum_{s=1}^{N_s}\lambda_s^{\nu}\sum_{i=1}^{N-\xi}\left(\frac{e_{it}e_{is}}{w_i A_i^3}\right)_{\nu} = \sum_{i=1}^{N-\xi}\frac{e_{it}}{A_i^{\nu}} - \eta(g_t^U - g_t^{\nu}) \; (t = 1, 2, ..., N_s)$$

Equations 20 and 21 together form an iterative algorithm to solve for the continuous design optimization problem posed in Equation 16. Given a set of sizing variables A_i^{ν}, the set of unknown Lagrange multipliers λ_s^{ν} is then determined by solving the linear simultaneous Equation 21. With the current values of λ_s^{ν}, the new set of sizing variables $A_i^{\nu+1}$ can then be sized using Equation 20. Such an iterative algorithm can be programmed to repeatedly solve for the sizing variables and the associated Lagrange multipliers until their convergence occurs. At convergence, the optimality criteria (Equation 19) are satisfied such that the optimal member sizes are obtained and the importance of each constraint to the optimal design are also determined by the final values of λ_s. Note that the optimization technique developed herein allows for simultaneous consideration of multiple sets of serviceability constraints involving the top building drift together with inter-story drifts and the translational periods as well as the rotational periods.

Once the continuous optimal solution is obtained, one needs to finalize the design with discrete standard sections. A pseudo-discrete OC technique[20] is herein adopted to achieve a smooth transition from the continuous variable design to the optimal final design using discrete standard sections. The essence of the pseudo-discrete OC technique is to maintain the least changes in the structure cost while members are progressively assigned standard section sizes. Details of the pseudo-discrete OC technique can be found in references 11 and 20.

Design Procedure

The procedure to implement the optimal design method for limiting lateral drifts and natural periods of tall steel building frameworks is listed as follows:

1) Analyze the structure under service wind loads and virtual loads.
2) Design members to satisfy strength requirements in accordance with a steel design standard and adopt the strength-based member size as the minimum size bound for each member.
3) Establish the explicit drift constraint Equation 7.
4) Perform an eigenvalue analysis to find the initial natural periods (T_o) and corresponding mode shapes (ϕ_o) for the framework.
5) Compute an inertia force $F = \omega_o^2 M\phi_o$ for each vibration mode and analyze statically the framework under inertia force, i.e. $F = K\phi$.
6) Compute the explicit equivalent period constraints Equation 15.
7) Combine both explicit drift and period constraints, and establish size bounds for members to form the explicit design optimization problem.
8) Apply the recursive optimization algorithm Equations 20 and 21 until optimal member sizes are obtained.
9) If the structure is statically indeterminate, return to step (1) to repeat the design process until the structure weight converges; otherwise, go to step 10.
10) Apply a pseudo-discrete section selection procedure to finalize the optimal design with discrete standard section sizes and terminate with the optimal building structure.

ILLUSTRATIVE EXAMPLES

Example 1: A 3-Bar Truss

A simple truss involving two diagonal members in two orthogonal directions and a common vertical column is shown in Figure 2. The purpose of this simple truss example is to illustrate the application of the optimization technique for minimum weight design involving multiple stiffness constraints. The truss is loaded at its top node by two lateral point loads taken as two separate loading conditions in the X and

Table 1. Analysis Results of the 3-Bar Truss							
Member	Actual Load		Virtual Load		Weight Coeff.	Energy Coeff.	
	F_{ix}	F_{iy}	f_{ix}	f_{iy}	$w_i = \rho_i L_i$	e_{ix}	e_{iy}
1	0	14.142	0	1.4142	14.142	0	2.8284
2	5.774	−10.000	0.5774	−1.000	10.000	0.3333	1.0000
3	−11.547	0	−1.1547	0	20.000	2.6667	0

Y orthogonal directions. The design objective is to minimize the structure weight subject to the two top drift constraints corresponding to the two respective X and Y direction loads. The structural geometry, material properties, and the two drift ratio limits at the top node are shown in Figure 2. Member sizes are assumed to be unbounded and nondimensional units of measurement are used for ease of illustration.

To facilitate the presentation, a subscript i denotes the member number, subscript x represents information pertaining to the X-direction load case and subscript y corresponds to the Y-direction load case. Results of the analysis of the statically determinate truss is shown in Table 1.

To commence the optimization process, an initial set of member sizes ($A_1^0 = A_2^0 = A_3^0 = 1$) is arbitrarily selected. Employing a step-size parameter $\eta = 2$, the set of simultaneous equation Equations 21 can be established to solve for the two Lagrange multipliers λ_x and λ_y, associated with the X and Y drift constraints. Once the current values of λ_x and λ_y are determined, the member sizes A_i can then be resized using the recursive relations Equations 20. Table 2 shows the results of the iterative design optimization process. Further details of the optimization technique for the solution of this example are given in Appendix A.

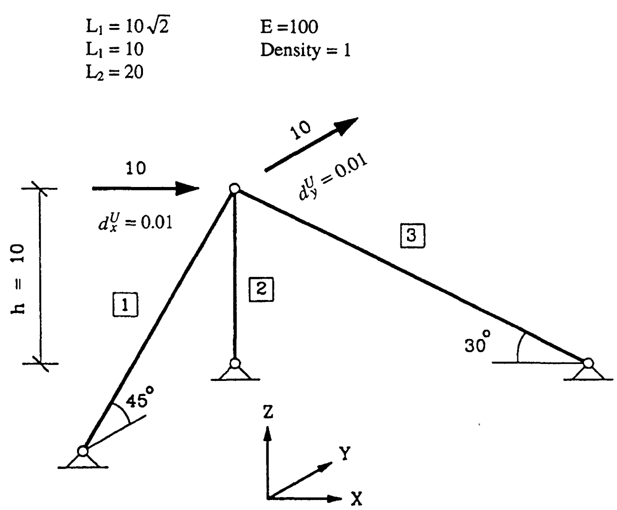

Fig. 2. Three-bar truss example.

The design process converges to the optimal structure weight of 1497.1 after ten iterations, where both the X and Y drift ratios are found reaching their limit of 0.01. By inspection, the 45° diagonal in the Y direction is structurally less efficient to resist lateral load than the 30° diagonal in the X-direction. Therefore, the truss is more vulnerable under the Y-direction load and the design is influenced more by the Y-direction drift. Such an intuition is evidently shown in Table 2, where the corresponding Lagrange multiplier has a larger value of $\lambda_y = 83481$ than the value of $\lambda_x = 66225$ for the X-direction drift. At the optimum of the design problem with multiple constraints, Table 3 shows that the weighted sum of the virtual energy densities for each member is equal to unity so as to satisfy the optimality criteria Equations 19 for the multiple drift constraint problem as shown in Table 3.

Example 2: A 50-story Building

A 50-story 7-bay by 10-bay practical building framework with 5400 members which is shown in Figure 3 and studied

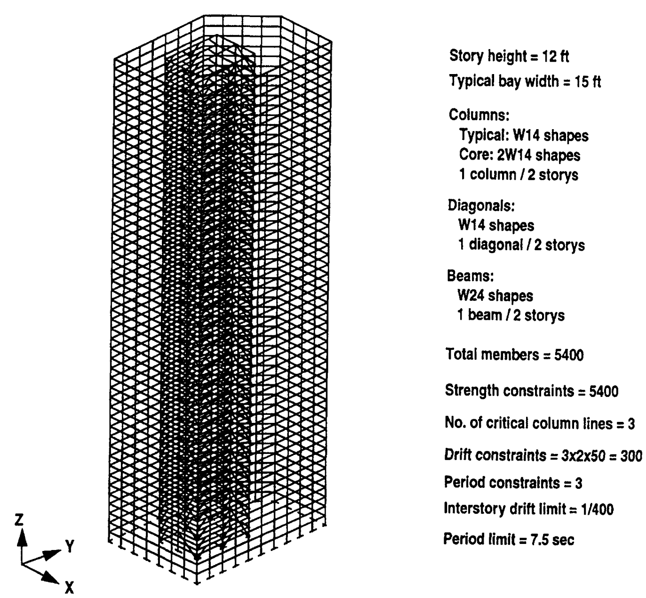

Fig. 3. 3D model of a 50-story framework.

Iteration ν	A_1^ν	A_2^ν	A_3^ν	g_x^ν	g_y^ν	Simultaneous Equation 21 L.H.S.		R.H.S.	λ_x^ν λ_x^ν	Structure Weight
0	1.000	1.000	1.000	0.30000	0.38284	3.6667E-03	3.3333E-04	0.8800	225.6	44.14
						3.3333E-04	6.6568E-03	1.1285	158.2	
1	2.082	1.667	2.004	0.15305	0.19581	4.6570E-04	7.1933E-05	0.4392	850.2	86.20
						7.1933E-05	8.4232E-04	0.5674	601.1	
2	3.928	3.486	3.830	0.07918	0.10070	6.5900E-05	7.8678E-06	0.2176	3037.7	167.01
						7.8678E-06	1.1697E-04	0.2821	2207.4	
3	7.584	6.361	7.202	0.04226	0.05302	9.9481E-06	1.2949E-06	0.1068	9758.8	314.92
						1.2949E-06	1.6853E-05	0.1390	7500.7	
4	13.682	11.633	12.634	0.02397	0.02927	1.8337E-06	2.1174E-07	0.0519	25781.6	562.51
						2.1174E-07	2.8438E-06	0.0678	21923.7	
5	22.865	18.933	19.921	0.01515	0.01765	4.6611E-07	4.9113E-08	0.0254	49395.6	911.11
						4.9113E-08	6.2058E-07	0.0330	49196.0	
6	32.949	26.807	26.491	0.01131	0.01232	1.9703E-07	1.7304E-08	0.0139	64078.1	1263.85
						1.7304E-08	2.1006E-07	0.0169	75385.4	
7	39.354	31.448	29.371	0.01014	0.01037	1.4390E-07	1.0717E-08	0.0104	66200.2	1458.46
						1.0717E-08	1.2497E-07	0.0111	83154.5	
8	40.807	32.453	29.712	0.01000	0.01001	1.3881E-07	9.7521E-09	0.0100	66225.4	1495.86
						9.7521E-09	1.1251E-07	0.0100	83480.6	
9	40.861	32.489	29.715	0.01000	0.01000	1.3875E-07	9.7198E-09	0.0100	66225.4	1497.06
						9.7198E-09	1.1208E-07	0.0100	83481.0	
10	40.861	32.489	29.715	0.01000	0.01000	1.3875E-07	9.7197E-09	0.0100	66225.4	1497.06
						9.7197E-09	1.1208E-07	0.0100	83481.0	

Table 2.
Iterative Optimization History for the 3-Bar Truss

in reference 11 for optimal static drift design is herein considered. The purpose of this example is to illustrate the effectiveness and practical application of the design automatic optimal sizing technique for large-scale 3D tall building frameworks subject to both static drift and dynamic natural period constraints. For a bay width of 4.57 m (15 ft) and a story height of 3.66 m (12 ft), the framework has a height-to-width aspect ratio of 5.7 in the X-direction and 4.0 in the Y-direction. Details of the framework are shown in its elevation and plan views in Figures 4 and 5. As illustrated in these figures, one corner of the building is cut off at a 45° angle and the core is eccentrically located in the Y-direction (i.e., shifted towards the south exterior face). These features create a built-in asymmetry that causes natural twisting of the framework under lateral loadings. The framework consists of exterior moment frames and a braced core. All beams and columns are rigidly connected while the diagonal braces are simply connected. As shown in Figure 4, two-story K-bracing modules are used on both the south and north faces of the core while single-story knee-bracing is used in the west and east faces of the core to ensure accessibility to the elevators in the core.

American AISC standard sections are used to size the members as follows: beams are W24 shapes; diagonals are W14 shapes; and columns are also W14 shapes except that the cruciform columns in the core (see Figure 5) use pairs of two W14 shapes oriented perpendicular to each other. To satisfy practical construction requirements, beams that are grouped together on each floor as shown in Figure 5 are specified to have the same section over two adjacent storys, while columns in each line are grouped together as having a common section over two adjacent storys, as are diagonals in each span. To establish the minimum size boundary for each member, member strength design is carried out after each response analysis process in accordance with the AISC LRFD design standard.[12] To account for serviceability lateral swaying and twisting of 1/400 is applied on all the columns at the most distant column lines A, B and C. For the control of dynamic wind-induced vibration, two lateral sway periods about the two orthogonal X and Y directions of the buildings are limited to 7.5 seconds respectively.

To study the practical application of the optimal design technique, three separate runs are conducted for this framework. The first run is to determine only member-by-member strength design for the structure. The second run considers the stiffness optimization subject to lateral drift constraints alone

Table 3. Optimality Criteria for the 3-Bar Truss						
$\lambda_x = 66225.4$ $\lambda_y = 83481.0$						
		Virtual Strain Energy		Virtual Strain Energy Density		Optimality Condition
Member i	Optimal A_i	$\frac{e_{ix}}{A_i}$	$\frac{e_{iy}}{A_i}$	$\frac{e_{ix}}{w_i A_i^2}$	$\frac{e_{iy}}{w_i A_i^2}$	$\lambda_x \frac{e_{ix}}{w_i a_i^2} + \lambda_y \frac{e_{iy}}{w_i A_i^2}$
1	40.861	0	6.922×10^{-3}	0	1.198×10^{-5}	0.000 + 1.000 = 1.000
2	32.489	1.026×10^{-3}	3.078×10^{-3}	3.158×10^{-6}	9.474×10^{-6}	0.209 + 0.791 = 1.000
3	29.715	8.974×10^{-3}	0	1.510×10^{-5}	0	1.000 + 0.000 = 1.000
Sum =		0.01000	0.01000			

while using strength-based sizes as the minimum size bounds. The last run is similar to the second run; but it includes both the static drift and the period constraints. For the last two stiffness design runs, a pseudo-discrete OC resizing technique[20] is applied upon convergence of the continuous optimization solution to finalize the design using discrete standard sections.

Rapid and steady convergence to the optimal design is found for all three design runs on this large-scale framework example. The history of the design process for the three runs of the framework is shown in Figure 6. For the first case where the structure is designed for strength alone, the structure results in a weight of 3848.8 tons. The optimal results of the other two stiffness design runs clearly indicate that the design of this framework is governed by lateral stiffness criteria rather than member strength requirements. An increase in structure weight to 5133.0 tons is found when only lateral drift constraints are considered. When both lateral drift and period constraints are involved in the design, an additional slight increase in structure weight to 5414.0 tons is found for the framework. Such a result indicates that the period constraints are more active to the design, or in other words, they control the design somewhat more than the drift constraints. As shown in Figure 6, all three runs exhibit stable and rapid

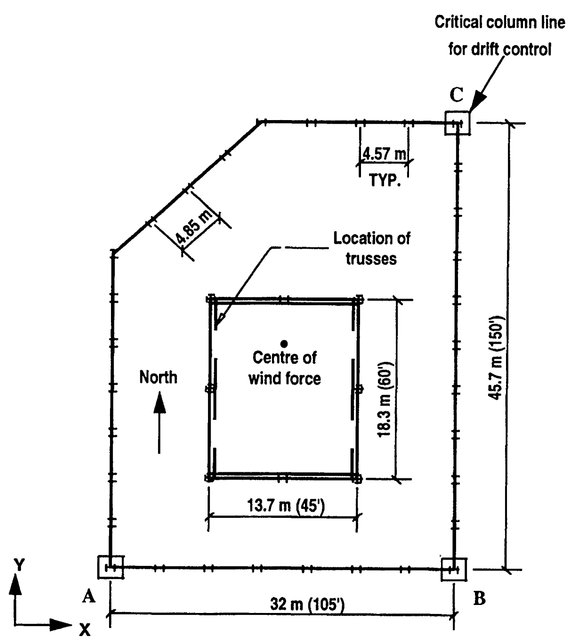

Fig. 4. Plan view of 50-story framework example.

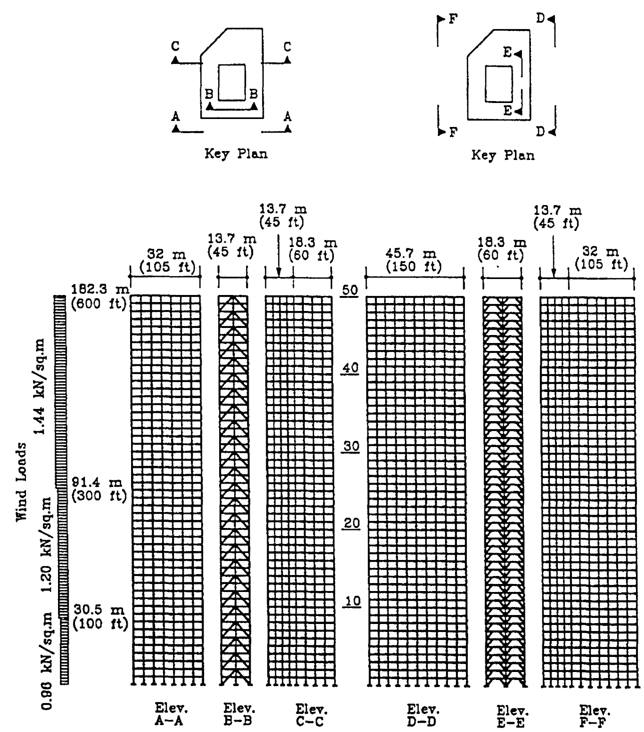

Fig. 5. Front and side elevations of 50-story framework example.

convergence. Such a quick convergence can be explained by the fact that the internal member force distribution is quite insensitive to changes in member sizes for building frameworks. Such a peculiar behavior of building frameworks results in good quality approximations of the explicit energy based stiffness constraints with consequent rapid convergence to the optimal design.

Figure 7 shows the deflected profiles of the framework in the two respective X and Y directions after completion of the design optimization process involving both lateral drift and period constraints. While the X-direction lateral response is controlled by drift constraints, the design in the Y-direction is governed by the corresponding sway period constraints. For the X-direction drift, the interstory drift ratios of the south-east and north-east corner column lines B and C above approximately the 10th floor are found active and are shown having a slope parallel to the drift ratio limit of $1/400$. A slight difference in lateral deflection of about 2.5 cm is found between the column line B and the column line C in the upper portion of the building, indicating a twisting rotation of 2.5 cm in 45.7 m or about $1/1800$ radian. Such a result seems to indicate that for the optimal design of an asymmetric framework, the lateral load resisting system will be sized by the OC procedure such as to distribute its stiffness so that little or no building torsion occurs. For the Y-direction lateral response, while lateral drifts are not active and no building twisting is shown, the sway period is found active with a value close to its limit of 7.5 sec. This result indicates that the optimal design technique may not necessarily end with a fully constrained design having all the constraints to reach their limits. Indeed, the automatic resizing technique will seek for the best response of the structure within the given set of design constraints such that the optimal objective for the design is achieved. As a result, the optimal design achieved may provide insights to engineers for further design improvements. Moreover, the design results obtained are often found to match closely our engineering intuition concerning the structural behaviour of building frameworks.

CONCLUDING REMARKS

An automatic resizing technique for the optimal stiffness design of tall steel building frameworks is presented in this paper. Based on the results presented in this paper, the following conclusions can be made:

1) Economy: Not only the most economical design is achieved by the optimal resizing technique while satisfying all design constraint requirements, but there is also a considerable saving in designer time and cost.
2) Effectiveness: Rapid and steady convergence is generally found since the formulation of the design problem using the energy approach has exploited to advantage the peculiar behavior of building framework, that the member force distributions for such structures are somewhat insensitive to changes in member sizes.
3) Practicality: The results of the three dimensional 50-story building example have demonstrated the practical application of the optimal design technique. The technique developed holds much promise for a powerful tool for the design of large-scale tall steel building frameworks encountered in professional practice.

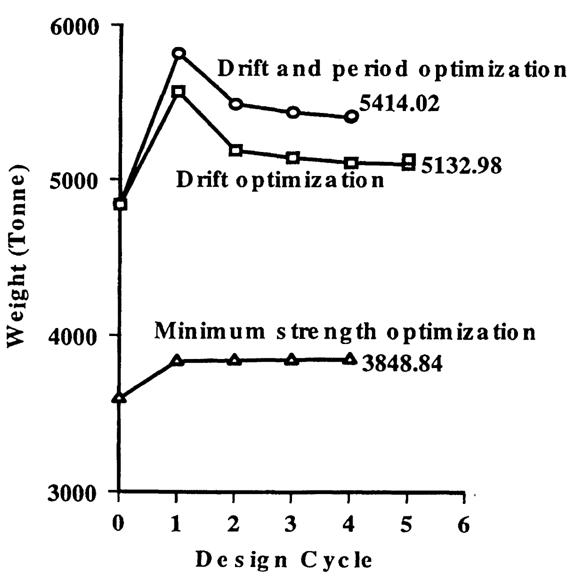

Fig. 6. Design history of 50-story framework example.

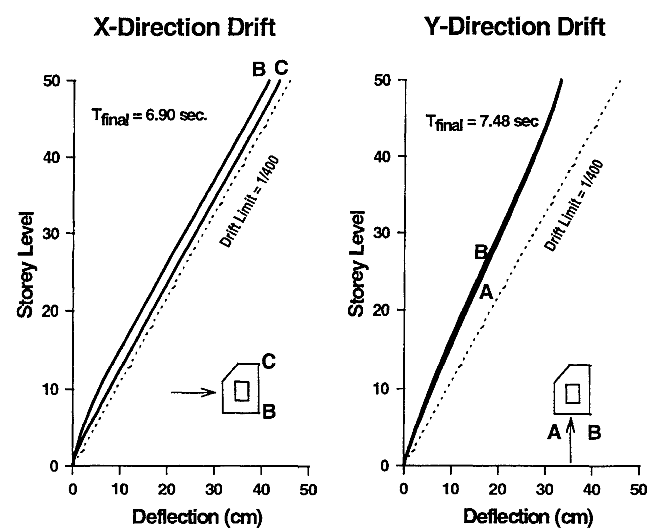

Fig. 7. Deflected profile for 50-story framework example.

ACKNOWLEDGEMENTS

The authors wish to thank the Hong Kong University of Science and Technology and the Research Grants Council of Hong Kong for providing financial support for this research.

REFERENCES

1. Council on Tall Buildings & Urban Habitat, *Structural Design of Tall Steel Buildings, Monograph on Planning and Design of Tall Buildings*, Vol. SB, Chapter SB-5, 1979.
2. Tallin, A. and Ellingwood, B., "Serviceability Limit States: Wind Induced Vibrations," ASCE, *Journal of Structural Engineering*, Vol. 110, No. 10, 1984, pp. 2424–2437.
3. Thorton, C. H., Joseph, L., and Scarangello, T. Z., "Optimization of Tall Structures for Wind Loading," *Journal of Wind Engineering and Industrial Aerodynamics*, Vol. 36, 1990, pp. 235–244.
4. Baker, W., "Sizing Techniques for Lateral Systems in Multi-Story Steel Buildings," *Proc. of the 4th World Congress on Tall Buildings*, Council on Tall Buildings and Urban Habitat, Hong Kong, 1990, pp. 875–868.
5. Charney, F. A., "The Use of Displacement Participation Factors in the Optimization of Wind Sensitive Buildings," *Proc. of the Ninth Structures Congress*, ASCE, Indianapolis, IN, 1991, pp. 545–547.
6. Gilsanz, R. and Carlson A., "Optimization in Building Design," *Proc. of the 2nd Int. Conf. on Computer Aided Optimum Design of Structures 91*, Hernandez S. and Brebbia C. A., eds., Boston, MA, 1991, pp. 481–492.
7. Khot, N. S., Berke, L., and Venkayya, V. B., "Comparison of Optimality Criteria Algorithms for Minimum Weight Design of Structures," *AIAA Journal*, Vol. 17, No. 2, 1979, pp. 182–190.
8. Khan, M. R., Willmert, K. D., and Thorton, W. A., "A New Optimality Criteria Method for Large Scale Structures," *Proc. AIAA/ASME/SAE 19th Struct. Dynamics and Mat. Conf.*, AIAA, Washington, D.C., 1978, pp. 47–58.
9. Zhou, M. and Rozvany, G. I. N., "DCOC: An Optimality Criteria Method for Large Systems: Part I: Theory," *Struct. Optimization*, Vol. 5, No. 1-2, 1992, pp. 12–25.
10. Chan, C. -M. and Grierson, G. E., "An Efficient Resizing Technique for the Design of Tall Steel Buildings Subject to Multiple Drift Constraints," *The Structural Design of Tall Buildings*, Vol. 2, 1993, pp. 17–32.
11. Chan, C. M., Grierson, D. E., and Sherbourne, A. N., "Automatic Optimal Design of Tall Steel Building Frameworks," *Journal of Structural Engineering*, ASCE, Vol. 121, No. 5, 1995, pp. 838–847.
12. American Institute of Steel Construction, *Manual of Steel Construction—Load and Resistance Factor Design*, 1st Ed., Chicago, IL, 1986.
13. Ad Hoc Committee on Serviceability Research, "Structural Serviceability: A Critical Appraisal and Research Needs," *Journal of Structural Engineering*, Vol. 112, No. 12, 1986, pp. 2646–2664.
14. ASCE Task Committee on Drift Control of Steel Building Structures, "Wind Drift Design of Steel-Framed Buildings: State-of-the-Art Report," *Journal of Structural Engineering*, Vol. 114, No. 9, 1988, pp. 2085–2108.
15. Ellingwood, B., "Serviceability Guidelines for Steel Structures," *Engineering Structures*, AISC, 1st Qtr., 1989, pp. 1–8.
16. Griffis, L., "Serviceability Limit States Under Wind Load," *Engineering Structures*, AISC, 1st Qtr., 1993, pp. 1–16.
17. Vickery, B. J., Isyumov, N., and Davenport, A. G., "The Role of Damping, Mass and Stiffness in the Reduction of Wind Effects on Structures," *Journal of Wind Engineering and Industrial Aerodynamics*, Vol. 11, 1983, pp. 285–294.
18. Henige, R. A., "Structural Optimization to Limit Natural Periods," *Proc. of Tenth Conf. on Electronic Computation*, Indianapolis, IN, April 29–May 1, 1991, pp. 253–260.
19. Briggs, J. M., *Introduction to Structural Dynamics*, McGraw-Hill Book Co., 1964.
20. Chan, C. -M., "A Pseudo-Discrete Optimization Technique for Tall Steel Building Design Using Standard Steel Sections," *Proc. of Int. Conf. on Advances in Steel Structures*, Hong Kong, Dec. 11–14, 1996, pp. 983–988.
21. Kirsch, U., *Structural Optimization—Fundamentals and Applications*, Springer-Verlag, Germany, 1993.
22. Templeman, A. B., *Civil Engineering Systems*, The Macmillan Press Ltd., 1982.
23. Morris, A. J., *Foundations of Structural Optimization: A Unified Approach*, John Wiley & Sons, 1982.
24. Pike, R. W., *Optimization for Engineering Systems*, Van Nostrand Reinhold Co., 1986.

APPENDIX A

This appendix describes further details of the OC optimization technique for the solution of the optimal drift design of the simple 3-bar truss example as shown in Figure 2. Given that the truss structure is statically determinate, member forces can be calculated independently of the member sizes and are listed in Table 1. Using the assumed values of the material density, the modulus of elasticity and member lengths shown in Figure 2, the strain energy coefficients in Equation 7 are calculated as

$$e_{1x} = \left(\frac{FfL}{E}\right)_{1x} \bullet \frac{1}{h} = \frac{0 \bullet 0 \bullet 10\sqrt{2}}{100} \bullet \frac{1}{10} = 0$$

$$e_{2x} = \left(\frac{FfL}{E}\right)_{2x} \bullet \frac{1}{h} = \frac{5.774 \bullet 0.5774 \bullet 10}{100} \bullet \frac{1}{10} = 0.03333$$

$$e_{3x}=\left(\frac{FfL}{E}\right)_{3x}\bullet\frac{1}{h}=\frac{-11.547\bullet -1.1547\bullet 20}{100}\bullet\frac{1}{10}$$

$$=0.26667$$

$$e_{1y}=\left(\frac{FfL}{E}\right)_{1y}\bullet\frac{1}{h}=\frac{14.142\bullet 14.142\bullet 10\sqrt{2}}{100}\bullet\frac{1}{10}=0.28284$$

$$e_{2y}=\left(\frac{FfL}{E}\right)_{2y}\bullet\frac{1}{h}=\frac{-10\bullet -1\bullet 10}{100}\bullet\frac{1}{10}=0.1$$

$$e_{3y}=\left(\frac{FfL}{E}\right)_{3y}\bullet\frac{1}{h}=\frac{0\bullet 0\bullet 20}{100}\bullet\frac{1}{10}=0$$

Note that since the structure is a truss, the correction coefficient terms e' in Equation 7 are equal to zero. Therefore, the X and Y drift constraints can be written as

$$g_x=\frac{e_{1x}}{A_1}+\frac{e_{2x}}{A_2}+\frac{e_{3x}}{A_3}=\frac{0.03333}{A_2}+\frac{0.26667}{A_3}\le 0.01$$

$$g_y=\frac{e_{1y}}{A_1}+\frac{e_{2y}}{A_2}+\frac{e_{3y}}{A_3}=\frac{0.028284}{A_1}+\frac{0.1}{A_2}\le 0.01$$

Using an initial set of member sizes $A_1^0 = A_2^0 = A_3^0 = 1$, the X and Y drift ratios can be obtained respectively as $g_x^0 = 0.3000$ and $g_y^0 = 0.38284$, which are found to violate the drift ratio limit of 0.01, indicating that the current design is too flexible.

With the current values of member sizes, the simultaneous linear equations for the two Lagrange multipliers λ_x and λ_y associated with the X and Y drift constraints can then be established. For the initial set of member sizes ($A_1^0 = A_2^0 = A_3^0 = 1$), the summation terms on the left hand side of the Equation 21 can be written as

$$\left(\sum_{i=1}^{3}\frac{e_{ix}e_{ix}}{w_iA_i^3}\right)_v=0+\frac{0.03333\bullet 0.03333}{10\bullet 1^3}+\frac{0.26667\bullet 0.26667}{20\bullet 1^3}$$

$$=3.6667\times10^{-3}$$

$$\left(\sum_{i=1}^{3}\frac{e_{ix}e_{iy}}{w_iA_i^3}\right)_v=0+\frac{0.03333\bullet 0.1}{10\bullet 1^3}+0=3.3333\times10^{-4}$$

$$\left(\sum_{i=1}^{3}\frac{e_{iy}e_{ix}}{w_iA_i^3}\right)_v=0+\frac{0.1\bullet 0.03333}{10\bullet 1^3}+0=3.3333\times10^{-4}$$

$$\left(\sum_{i=1}^{3}\frac{e_{iy}e_{iy}}{w_iA_i^3}\right)_v=\frac{0.28284\bullet 0.28284}{10\sqrt{2}\bullet 1^3}+\frac{0.1\bullet 0.1}{10\bullet 1^3}+0$$

$$=6.6568\times10^{-3}$$

Employing a step-size parameter $\eta = 2$, the right hand side of Equation 21 is obtained as

$$\sum_{i=1}^{3}\frac{e_{ix}}{A_i^0}-\eta(d_x^U-d_x^0)=0.3-2(0.01-0.3)=0.880$$

$$\sum_{i=1}^{3}\frac{e_{iy}}{A_i^0}-\eta(d_y^U-d_y^0)=0.382843-2(0.01-0.382843)$$

$$=1.1285$$

Therefore, the simultaneous equations Equation 21 in terms of λ_x^0 and λ_y^0 can be expressed as

$$\begin{bmatrix}3.6667\times10^{-3} & 3.3333\times10^{-4}\\ 3.3333\times10^{-4} & 6.6568\times10^{-3}\end{bmatrix}\begin{bmatrix}\lambda_x^0\\ \lambda_y^0\end{bmatrix}=\begin{bmatrix}0.8800\\ 1.1285\end{bmatrix}$$

Solving the above simultaneous equation, the Lagrange multipliers are found such that

$\lambda_x^0 = 225.62$ and $\lambda_y^0 = 158.23$.

Having obtained λ_x^0 and λ_y^0, a new set of member sizes can be found from the recursive relationships of Equation 20 as

$$A_1^1=A_1^0\left[1+\frac{1}{\eta}\left(\sum_{s=1}^{2}\lambda_s\frac{e_{1s}}{w_1A_1^2}-1\right)\right]_0$$

$$=1\left[1+\frac{1}{2}\left(225.62\bullet\frac{0}{10\sqrt{2}\bullet 1^2}+158.23\bullet\frac{0.28285}{10\sqrt{2}\bullet 1^2}-1\right)\right]$$

$$=2.082$$

$$A_2^1=A_2^0\left[1+\frac{1}{\eta}\left(\sum_{s=1}^{2}\lambda_s\frac{e_{2s}}{w_2A_2^2}-1\right)\right]_0$$

$$=1\left[1+\frac{1}{2}\left(225.62\bullet\frac{0.03333}{10\bullet 1^2}+158.23\bullet\frac{0.1}{10\bullet 1^2}-1\right)\right]$$

$$=1.667$$

$$A_3^1=A_3^0\left[1+\frac{1}{\eta}\left(\sum_{s=1}^{2}\lambda_s\frac{e_{3s}}{w_3A_3^2}-1\right)\right]_0$$

$$=1\left[1+\frac{1}{2}\left(225.62\bullet\frac{0.26667}{20\bullet 1^2}+158.23\bullet\frac{0}{20\bullet 1^2}-1\right)\right]$$

$$=2.004$$

After obtaining the new set of member sizes as in the foregoing, the OC process is repeated in an iterative fashion until convergence of both member sizes and Lagrange multipliers occurs. The iteration history of the OC optimization process for the truss design is tabulated in Table 2.